V International Conference on Computational Methods for Coupled Problems in Science and Engineering
COUPLED PROBLEMS 2013
S. Idelsohn, M. Papadrakakis and B. Schrefler (Eds)

AN IMMERSED BOUNDARY LEVEL-SET BASED APPROACH FOR FLUID-SHELL INTERACTION WITH IMPACT

RODOLFO A. K. SANCHES*, ROGÉRIO CARRAZEDO* AND HUMBERTO B. CODA†

*Academic Department of Civil Engineering
Universidade Tecnológica Federal do Paraná (UTFPR)
Campus de Pato Branco, via do conhecimento Km 1, Pato Branco PR, Brazil
e-mail: rodolfosanches@utfpr.edu.br, web page: http://www.pb.utfpr.edu.br/ecv/

†Structural Engineering Department of São Carlos Engineering School
University of São Paulo (USP)
Campus de São Carlos, Av. do Trabalhador Sãocarlense, 400, São Carlos, SP, Brazil
e-mail: hbcoda@sc.usp.br - Web page: http://www.set.eesc.usp.br/

Key words: Fluid shell interaction, Embedded coupling, large displacement, geometric nonlinear shell dynamics, Finite elements

Abstract. Fluid-shell interaction modeling is a challenging problem with application to several engineering fields. In this research we develop a partitioned algorithm for large displacements fluid-shell coupling with impact. The structure is modeled in a total Lagrangian description, using a novel shell finite element formulation to deal with geometric nonlinear dynamics of thin or thick shells. This formulation is based on the principle of minimum potential energy considering positions and generalized unconstrained vectors as nodal parameters, instead of displacements and rotations. As a consequence, the formulation eliminates the need for large rotation approximations and presents constant mass matrix, allowing the use of Newmark time integrator for the nonlinear problem. The Newton-Raphson method is employed to solve the resulting nonlinear system and contact between structures is modeled by enforcing non-penetration conditions based on a signed distance function. The flow is assumed to be compressible and the fluid dynamics solver is explicit with time integration based on characteristics. The fluid governing equations are written in the Eulerian description generating a fixed mesh method. The coupled problem is solved by using an embedded boundary technique where the fluid-shell interface is tracked inside the unstructured fluid mesh by level sets of a signed distance to boundary function. The versatility and efficiency of the proposed approach is demonstrated by selected three- dimensional examples.

1 INTRODUCTION

Fluid structure interaction problems are found in various engineering activities, such as civil buildings, mechanical devices, aeronautics, ocean structures and biomechanics. Many of these problems can be modeled as shell structures interacting with compressible flows and are a challenging field, specially if contact/impact may occur.

Mathematical modeling of mechanical problems is traditionally done in a Lagrangian or in a Eulerian description. Lagrangian description expresses the continuum medium movement in terms of the initial configuration and time, being very efficient for problems where finite displacements are the main variables, such as in solid mechanics. On the other hand, the Eulerian description is defined in terms of final configuration and time, being well used for problems where the variables are velocities instead of displacements, such as for fluid mechanics.

Both fluid and solid mechanics are involved in the study of fluid-structure interaction problems, implying the need to couple Eulerian description to Lagrangian description. One widely used way to deal with such situations is to solve the solid based on a Lagrangian description and the fluid based on an Arbitrary Lagrangian-Eulerian (ALE) description, in which an arbitrary velocity may be applied to the reference domain.

Using ALE description for Navier-Stokes equations together with some mesh moving technique is a methodology able to deal with many fluid-structure interaction problems [10, 3, 9]. However, some problems of large scale of displacements, such as air-bag or parachute deployment, will require also a remesh technique if the ALE description is employed.

Some authors have proposed immersed methods for Eulerian-Lagrangian coupling, most of them in the finite difference context, considering immersed boundary in a structured mesh [1, 4, 6].

The technique proposed here for coupling the Lagrangian shell finite element solver to the Eulerian fluid finite element solver considers the shell boundary moving inside the fluid unstructured mesh in which it is immersed. The shell position is tracked with level sets of a boundary signed distance function, and the fluid Dirichlet boundary conditions are applied by enforcing a ghost flow over the nodes immediately outside the shell boundary and, at same time, limiting the velocity slope based on the signed distance function. Shell-Shell multi-body contact is modeled by imposing non-penetration conditions based on a body to body signed distance function.

The outline of the paper consists in first briefly describe shell and fluid formulations, then describe the coupling algorithm and the impact algorithm, and finally present examples of inflatable structure problems giving a qualitative demonstration of feasibility and quality of the proposed technique.

2 SHELL FORMULATION

Shell structures are solids with one dimension much larger than the others. Therefore, the mid surface serves as a reference to the solid mapping. The mappings f^0 and f^1, from an auxiliary non-dimensional space respectively to the initial and current configurations may be written as follows:

For any point out of the middle surface, its position at initial and final configuration may be written as:

$$f_i^0 = X_i = N_j(\xi_1, \xi_2) X_{ji}^m + \frac{h_0}{2} \xi_3 N_j(\xi_1, \xi_2) e_{ij}^0, \tag{1}$$

and

$$f_i^1 = x_i = N_j(\xi_1, \xi_2) x_{ji}^m + \frac{h_0}{2} \left[\xi_3 + a_j N_j(\xi_1, \xi_2) \xi_3^2\right] \; N_j(\xi_1, \xi_2) \, \bar{G}_{ij}, \tag{2}$$

where $\bar{G}_{ij}$ are the nodal values (unknowns) for the generalized vector at node j at final configuration, h^0 is the initial thickness, e_i^0 is the $i-th$ component of the unitary vector $\overrightarrow{e^0}$, normal to the midle surface at initial and a is the strain rate along thickness.

Finally, change of configuration from initial to current is represented by:

$$\mathbf{f} = \mathbf{f}\left(\mathbf{X}\right) = \left(\mathbf{f}^1\right) \circ \left(\mathbf{f}^0\right)^{-1}. \tag{3}$$

The gradient $\mathbf{A}$ of the configuration change function may be expressed by:

$$\mathbf{A} = \nabla \mathbf{f} = \left(\mathbf{A}^1\right) \left(\mathbf{A}^0\right)^{-1}. \tag{4}$$

After evaluating the gradient $\mathbf{A}$, the Green strain tensor and the specific strain energy may be obtained, following [8]:

$$E_{ij} = \frac{1}{2} \left[A_{ki} A_{kj} - \delta_{ij}\right] = \frac{1}{2} \left[C_{ij} - \delta_{ij}\right]. \tag{5}$$

The variables C_{ij} and δ_{ij} are the right Cauchy-Green stretch tensor and the Kroenecker delta, respectively. The following quadratic strain energy per unit of initial volume is adopted,

$$u_e = \frac{1}{2} E_{ij} C_{ijkl} E_{kl} \tag{6}$$

resulting into a linear elastic constitutive law relating second Piola-Kirchhoff stress and Green strain, usually called Saint-Venant–Kirchhoff elastic law, i.e.:

$$S_{ij} = \frac{\partial u_e}{\partial E_{ij}} = C_{ijkl} E_{kl} \tag{7}$$

where The C_{ijkl} are the components of the elastic constants tensor.

From preceding developments, one may write the equilibrium equation as the minimization of the energy functional as:

$$\frac{\partial \mathbf{U_e}}{\partial x} - \mathbf{F} + \mathbf{M}\ddot{\mathbf{x}} + \mathbf{C}\dot{\mathbf{x}} = 0, \tag{8}$$

where $\mathbf{F}$ is the external forces vector, C is the dissipative matrix and $\mathbf{M}$ is the mass matrix.

[2] proved that for a positional total Lagrangian description, the Newmark β with $\gamma = 1/2$ presents momentum conservative properties for most of shell dynamics problems and conserves energy for small strains if the time step is sufficiently large that the asymptotic energy convergence dominates or small enough that a uniform bound on the energy is achieved (see [5] for more details with respect to energy conservation for constant mass matrix nonlinear dynamics with the average acceleration time integration).

From Newmark β method, the equilibrium equation for a given instant $s+1$ becomes:

$$\left.\frac{\partial \mathbf{U}_e}{\partial x}\right|_{S+1} - \mathbf{F}_{S+1} + \frac{\mathbf{M}}{\beta \Delta t^2}\mathbf{x}_{S+1} - \mathbf{M}\mathbf{Q}_S + \mathbf{C}\mathbf{R}_S + \frac{\gamma \mathbf{C}}{\beta \Delta t}\mathbf{x}_{S+1} - \gamma \Delta t \mathbf{C}\mathbf{Q}_S = 0, \tag{9}$$

where $\mathbf{Q}_S = \frac{\mathbf{x}_S}{\beta \Delta t^2} + \frac{\dot{\mathbf{x}}_S}{\beta \Delta t} + \left(\frac{1}{2\beta} - 1\right)\ddot{\mathbf{x}}_S$ and $\mathbf{R}_S = \dot{\mathbf{x}}_S + \Delta t\,(1-\gamma)\,\ddot{\mathbf{x}}_S$.

Equation (9) represents a nonlinear system, which we solve employing Newton-Raphson method. Each node will have 7 nodal parameters: 3 position vector components x_i with $i = 1, 2$ or 3, 3 components of the generalized position vector $\bar{G}_i$ with $i = 1, 2$ or 3 and the strain ratio along thickness a.

3 FEM FOR FLUID DYNAMICS

If there is no diffusion, the time variation of ϕ over a characteristic coordinates x' is by definition null. For the Navier-Stokes equations we can write:

$$\frac{\partial \phi(x', t)}{\partial t} - Q(x') = 0, \tag{10}$$

where $Q(x')$ contains all the non convective terms.

We assume the following approximation for Eq. (10) [11]:

$$\frac{\phi(y)_{n+1} - \phi(x)_n}{\Delta t} \approx \theta(Q(y)_{n+1}) + (1-\theta)(Q(x)_n), \tag{11}$$

where x and y means respectively the characteristic positions at $t = n$ and $t = n+1$, θ is a constant with value 0 for explicit solution and may be chosen larger than zero 0 and smaller than 1 for semi-implicit or implicit solution.

The product $u\phi$ and the term $Q(x)$ may be approximated by Taylor resulting the following expressions:

$$u\phi(x)_n = u\phi(y)_n - (y-x)\frac{\partial(u\phi(y))_n}{\partial x} + \frac{(y-x)^2}{2}\frac{\partial^2(u\phi(y)_n)}{\partial x^2} + O(\Delta t^3), \tag{12}$$

$$Q(x)_n = Q(y)_n - (y-x)\frac{\partial Q(y)_n}{\partial x} + O(\Delta t^2). \tag{13}$$

Assuming $\Delta t = (y-x)/u$, from Eqs. (12), (11) and (13), and assuming $\theta = 0$ (explicit form), we have:

$$\begin{aligned}\phi(y)_{n+1} = \phi(y)_n - \Delta t\left(\frac{\partial(u\phi(y))_n}{\partial x} - Q(y)_n\right) \\ + \frac{(\Delta t)^2}{2}u\frac{\partial}{\partial x}\left(\frac{\partial(u\phi(y)_n)}{\partial x} - Q(y)_n\right) + O(\Delta t^2).\end{aligned} \tag{14}$$

One important point about this procedure is that the high order terms of Eq. (14), obtained due to time integration along characteristics, introduce dissipation on stream lines direction, which as shown by [11] are equivalent to the Petrov-Galerking schemes when the time interval tends to the critical time interval, and gets smaller effects as the time interval get larger.

Applying the procedure of Eq. (14) to the Navier-Stokes equations, one may write for momentum and energy equations one may write:

$$\begin{aligned}\Delta(\rho u_i)_{n+1} = \Delta t\left(-\frac{\partial(u_j\rho u_i)}{\partial x_j} + \frac{\partial\tau_{ij}}{\partial x_j} - \frac{\partial p}{\partial x_i} + \rho g_i\right)_n + \\ \frac{\Delta t^2}{2}\left(u_k\frac{\partial}{\partial x_k}\left(\frac{\partial(u_j\rho u_i)}{\partial x_j} - \frac{\partial\tau_{ij}}{\partial x_j} + \frac{\partial p}{\partial x_i} - \rho g_i\right)\right)_n\end{aligned} \tag{15}$$

and

$$\begin{aligned}\Delta(\rho E)_{n+1} = \Delta t\left(-\frac{\partial(u_i\rho E)}{\partial x_i} + \frac{\partial}{\partial x_i}\left(k\frac{\partial T}{\partial x_i}\right) - \frac{\partial(u_i p)}{\partial x_i} + \frac{\partial(\tau_{ij}u_j)}{\partial x_i} - \rho g_i u_i\right) + \\ \frac{\Delta t^2}{2}u_k\frac{\partial}{\partial x_k}\left(\frac{\partial(u_i\rho E)}{\partial x_i}\right) + \\ \frac{\Delta t^2}{2}u_k\frac{\partial}{\partial x_k}\left(-\frac{\partial}{\partial x_i}\left(k\frac{\partial T}{\partial x_i}\right) + \frac{\partial(u_i p)}{\partial x_i} - \frac{\partial(\tau_{ij}u_j)}{\partial x_i} + \rho g_i u_i\right)_n,\end{aligned} \tag{16}$$

where all the right hand side terms are known at the instant $t = n$.

Based on the Eulerian mass conservation equation, [11] suggest the following expression for explicit solution:

$$\Delta\rho_{n+1} = -\Delta t\frac{\partial\left(\rho u_i\right)_{n+\theta}}{\partial x_i} = -\Delta t\left(\frac{\partial}{\partial x_i}\left(\rho u_i\right)_n + \theta\frac{\partial\left(\Delta\left(\rho u_i\right)\right)_{n+1}}{\partial x_i}\right), \tag{17}$$

where θ is a arbitrary constant with value between 0.5 and 1.

Applying the Galerkin method to Eq. (15), (17) and (16), we obtain the spatial discretization and solve the resulting system getting the week solution.

We still need to deal with the discontinuities due to the presence of shock waves, as the standard Galerkin method is unable to deal with strong discontinuities. Therefore, the artificial diffusion term based on pressure second derivative is added:

$$f_{\mu_a} = \Delta t \mu_a \frac{\partial}{\partial x_i}\left(\frac{\partial \phi}{\partial x_i}\right), \tag{18}$$

where ϕ is the variable to be smoothed and μ_a is the artificial viscosity given by:

$$\mu_a = q_{dif} h^3 \frac{(|\mathrm{u}| + c)}{p_{av}} \left| \frac{\partial}{\partial x_i}\left(\frac{\partial p}{\partial x_i}\right)\right|_e, \tag{19}$$

where $|\mathrm{u}|$ is the velocity absolute value, p_{av} is the pressure average over the element, q_{dif} is an user specified coefficient taken between 0 and 2, c is the sound speed and h is the element size [11, 7].

4 IMMERSED FLUID-STRUCTURE COUPLING PROCEDURE

The proposed method for enforcing boundary conditions on the vicinity of a shell immered in an unstructured fluid mesh requires all the fluid elements close to the boundary Γ_s to be identified, and to know if they are inside or outside the physical domain Ω_f. To this end, a computationally efficient and scalable approach is to use a signed distance function (or, level set function):

$$\Phi(x,\Gamma) = \begin{cases} \text{distance}(x,\Gamma) & \text{if } x \in \Omega \\ 0 & \text{if} x \in \Gamma \\ -\text{distance}(x,\Gamma) & \text{otherwise} \end{cases} \tag{20}$$

whose zero-th level set determines the resulting body shape.

In contrast to the usual parametric mesh based boundary representations (using segments or facets), level set based representations are more suitable for problems with large deformations and topology changes. There are efficient and scalable algorithms for converting a mesh based representation into an implicit representation.

Next, all the fluid elements are tagged as *physical*, *fictitious* or *boundary* depending on their position with respect to the physical domain. This classification is performed by computing for each fluid element Ω_{ef} the minimum and maximum signed distance $\min \Phi(\Omega_{ef})$ and $\max \Phi(\Omega_{ef})$, respectively, then the classification is applied as (see Fig. 1):

- physical element: $\min \Phi(\Omega_e) > 0$;
- fictitious element: $\max \Phi(\Omega_e) \leq 0$;

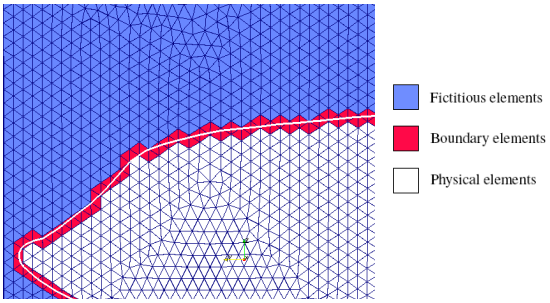

Figure 1: Elements tags

- boundary element: neither a physical nor a fictitious element.

The purpose of the element tag is to identify which nodes and elements should be deactivated from the analysis as well as the ghost nodes. To this purpose, all the fluid mesh nodes are tagged as *active* or *inactive*. A node k is active if $\Phi(k) > 0$ or if k bellows to some boundary fluid element, and inactive otherwise.This tags are computed for each time step and the inactive nodes as well as the fictitious elements are deactivated from the analysis.

For each fluid node k, we find the closest point l on shell mesh, and store the shell element Ω_{se} for which $l \in \Omega_{se}$ and the non-dimensional shell coordinates (ξ_1, ξ_2) for point l.

The active nodes k outside the physical domain ($\Phi(k) < 0$) need to be populated. For this purpose we project the point k to the closest physical element determining a new point m from where the values of density, specific energy and momentum are linearly extrapolated.

A way to prescribe the velocity at the boundary position would be to change the velocity nodal values of the active nodes k with $\Phi(k) < 0$ (ghost nodes) in order to modify the values over the boundary. However this procedure may imply on very large velocity values as $\Phi(k)$ becomes close to the element size.

To avoid this problem, we modify the velocity nodal values for the active nodes outside the boundary and also the velocity nodal inside a strip of width δ according to the following equation if the flow is inviscid:

$$\mathbf{u}_f = \mathbf{u}_f + (1 - \frac{\Phi}{\delta})[(\mathbf{u}_s - \mathbf{u}_f) \cdot \mathbf{n}]\mathbf{n}. \tag{21}$$

or, for a viscous flow:

$$\mathbf{u}_f = \mathbf{u}_f + (1 - \frac{\Phi}{\delta})[\mathbf{u}_s - \mathbf{u}_f] \tag{22}$$

where $\mathbf{u}_f$ is the fluid nodal fluid velocity vector, $\mathbf{u}_s$ is the shell velocity vector evaluated at the shell closest point to the fluid node. The term $(1 - \frac{\Phi}{\delta})$ limits the slope of velocity on

direction normal to the boundary but also introduces an artificial stiffness to the problem. However if we adopt a δ equal to the element size, this artificial stiffness is equal to the one naturally produced by an mesh of same elements size adapted to the boundary.

Taking advantage of the fluid shape functions, the stress tensor may be evaluated directly over the position of the embedded shell nodes k or directly over the shell quadrature points. the shell loads with respect to the Cartesian axes are given by:

$$q_{kj} = \left[-\tau_{jl} n_l - p n_l\right]_{Pf_k}, \tag{23}$$

where the indexes j and l represent Cartesian direction and n_l is the l component form the normal vector to Γ_s.

5 SHELL-SHELL CONTACT

Contact between structures is modeled by enforcing non-penetration conditions based on a body-body signed distance function.

Each Newton-Raphson iteration, over each body i, we calculate the signed distance to the other bodies k nodal values $\Phi_{si}(k)$. This value is positive if the node did not cross other bodies, regarding its initial position, or negative if it crossed.

If the value is negative, the node position is projected back a distance of $\frac{\Phi_{si}}{2}$ along its normal direction (slip wall contact). this procedure is repeated after each Newton-Raphson iteration until reach the prescribed error.

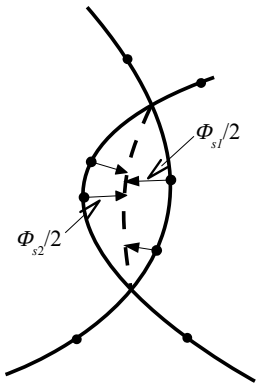

Figure 2: Contact

6 NUMERICAL EXAMPLE

In this example a simulation of an airbag deployment and crash with an half sphere moving on the airbag direction. We consider it as a qualitative example, once due to computational the airbag mesh is not fine enough to represent the wrinkles that appears

in high frequency and also because the formulation is not yet ready to simulate self contact, what is common in a problem like this. The airbag on its flat initial condition is filled

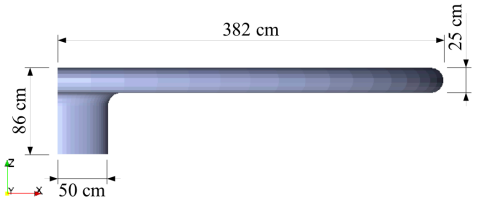

Figure 3: One quarter of the airbag

with an ideal gas at rest with density $\rho_f = 1.3kg/m^3$ pressure $p = 107,34kPa$ and specific heat ratio $\gamma = 1.4$. A gas with $\rho_{fi} = 10kg/m^3$, sound speed $c = 370m/s$ and $\gamma = 1.4$ enters the airbag producing a shock wave.

The input condition is kept constant until $t = 0.06\ s$, when the input is closed and the applied boundary condition is that of slip wall. The fluid mesh where the airbag is immersed has 263667 elements and 47491 nodes.

We discretize 1/4 of the problem assuming that the problem is symmetric according to the planes xz and yz and. The airbag is discretized by 258 elements and 1237 nodes and its material has Young's modulus $E = 3GPa$ and specific mass $\rho_s = 1000kg/m^3$ and thickness $h = 0.5mm$. The aibag is clamped over all the input area and simmetry boundary conditions are applied to the planes xz and yz.

A half sphere with specific mass $\rho_{s2} = 3000kg/m$, thickness $h = 15mm$ and Young's modulus $E = 20GPa$ is initially positioned at $z =$ and moves on the airbag direction with a speed $w = -25m/s$. The 1/4 of the half sphere is discretized by 6 curved elements and 37 nodes.

The simulation produced results according to the expectations. Figure 4 plots the top displacement versus time and figure 5 presents a snapshots of pressure distribution and the airbag deformation for some instants.

From these results we conclude that the present procedure is a robust method for analysis of inflatable structures and should further be improved to enlarge computing capabilities and shell self contact.

7 CONCLUSION

We have proposed one numerical model for analysis of shell high-speed flows coupling and for impact between shell structures. We presented the shell solver, which is able to deal with geometrical nonlinear dynamics of shells and uses a methodology based on the minimum potential energy theorem written regarding nodal positions and generalized unconstrained vectors, not displacements and rotations, avoiding the use of large rotation

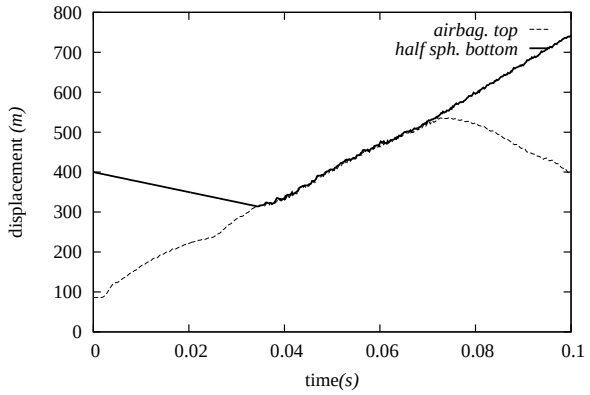

Figure 4: Top vertical displacements vs. time

approximations. The resulting time integration is stable for problems like the example presented here and based on the Newmark method due to the presence of constant mass matrix. Finally we developed the coupling procedure. The immersed approach furnishes a general algorithm for explicit coupling of Lagrangian shell solvers with unstructured-mesh-based Eulerian fluid solvers considering the shell immersed in a block of unstructured fluid mesh.The coupled algorithms are tested by one selected example. The employed fluid and shell solver showed to be robust and completely adequate for simulating fluid-shell interaction with impact. Further improvements on computer capability and shell self contact are recommended.

Acknowledgments

The authors would like to thank the Brazilian council CNPq (*Conselho Nacional de Desenvolvimento Cientfico e Tecnolgico*) and the State of Paran Foundation *Fundao Araucria* for the financial support.

REFERENCES

[1] F. Cirak and R. Radovitzky. A lagrangian-eulerian shell-fluid coupling algorithm based on level sets. *Computers & Structures*, 83(6-7):491 – 498, 2005. Frontier of Multi-Phase Flow Analysis and Fluid-Structure.

[2] H. B. Coda and R. R. Paccola. Unconstrained Finite Element for Geometrical Nonlinear Dynamics of Shells. *Mathematical problems in engineering*, 2009.

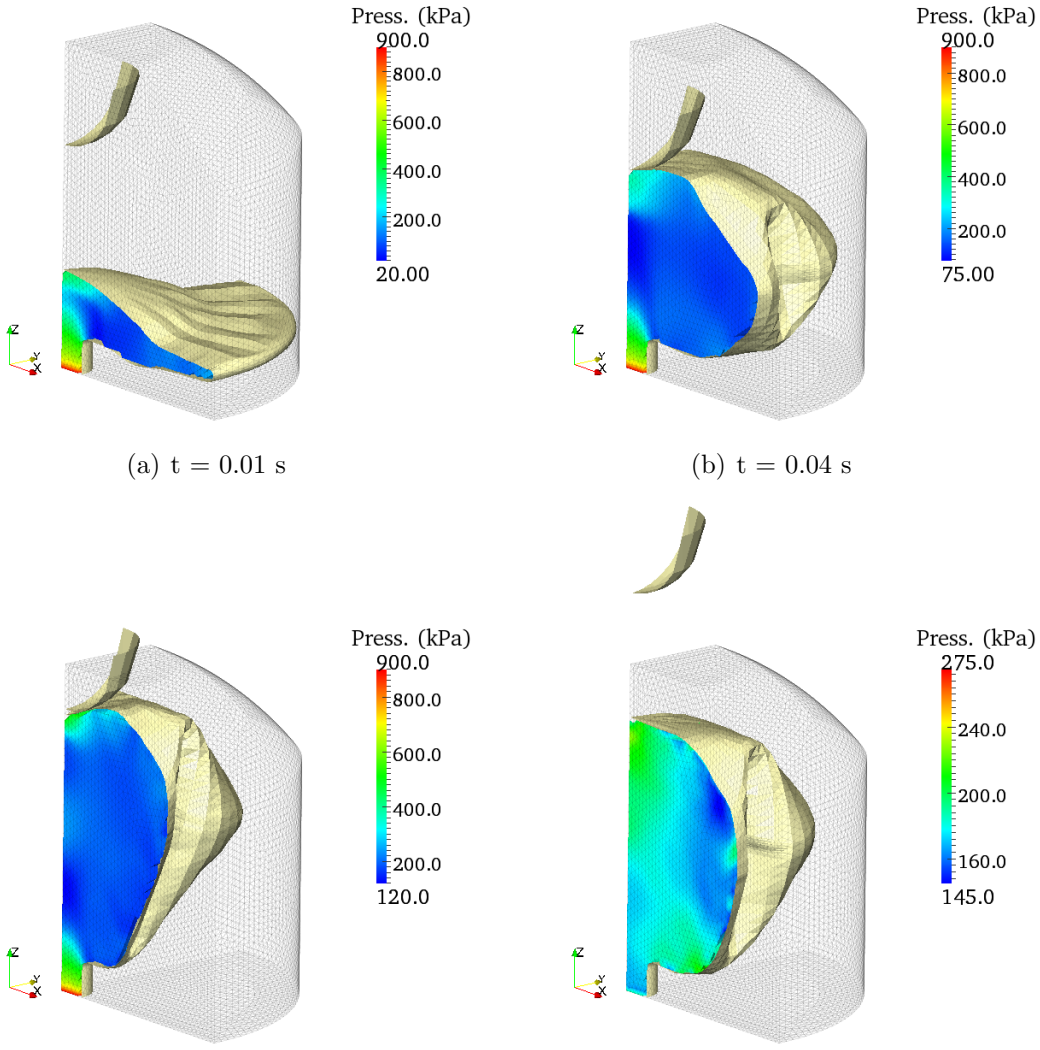

(a) t = 0.01 s

(b) t = 0.04 s

(c) t = 0.06 s

(d) t = 0.09 s

Figure 5: Pressure snapshots

[3] J. Donea, S. Giuliani, and J.P. Halleux. An arbitrary lagrangian-eulerian finite element method for transient dynamic fluid-structure interactions. *Computer Methods in Applied Mechanics and Engineering*, 33(1-3):689 – 723, 1982.

[4] F. Habbal. *The Optimal Transportation Meshfree Method for General Fluid Flows and Strongly Coupled Fluid-Structure Interaction Problems*. Phd thesis, California

Institute of Technology, Pasadena, California, 2009.

[5] T.J.R. Hughes. Stability, convergence and growth and decay of energy of the average acceleration method in nonlinear structural dynamics. *Computers & Structures*, 6(4-5):313 – 324, 1976.

[6] E. Morano M. Arienti, P. Hung and J.E. Shepherd. A level set approach to eulerian-lagrangian coupling. Technical report, California Institute of Technology, Pasadena, California, 2008. Caltech ASCI technical report 136.

[7] P Nithiarasu, OC Zienkiewicz, BVKS Sai, K Morgan, R Codina, and M Vazquez. Shock capturing viscosities for the general fluid mechanics algorithm. *International Journal for Numerical Methods in Engineering*, 28(9):1325–1353, Dec 15 1998.

[8] R.W. Ogden. Non-linear elastic deformations. *Engineering Analysis*, 1(2):119 – 119, 1984.

[9] T. Sawada and T. Hisada. Fluid-structure interaction analysis of the two-dimensional flag-in-wind problem by an interface-tracking ale finite element method. *Computers & Fluids*, 36(1):136 – 146, 2007. Challenges and Advances in Flow Simulation and Modeling.

[10] A. Soria and F. Casadei. Arbitrary Lagrangian-Eulerian multicomponent compressible flow with fluid-structure interaction. *International Journal for Numerical Methods in Fluids*, 25(11):1263–1284, 1997.

[11] O. C. Zienkiewicz and R. L. Taylor. *The Finite Element Method, v3: Fluid Dynamics*. Butterworth-heinemann Linacre house, 2000.